The Rupture Process of the Mw 7.8 Cape Kronotsky, Kamchatka, Earthquake of 5 December 1997 and Its Relationship to Foreshocks and Aftershocks

Article *in* Bulletin of the Seismological Society of America · December 2001

DOI: 10.1785/0119990116

CITATIONS
23

READS
70

1 author:

Vyacheslav Zobin
Universidad de Colima
223 PUBLICATIONS **1,103** CITATIONS

SEE PROFILE

Bulletin of the Seismological Society of America, 91, 6, pp. 1619–1628, December 2001

The Rupture Process of the M_w 7.8 Cape Kronotsky, Kamchatka, Earthquake of 5 December 1997 and Its Relationship to Foreshocks and Aftershocks

by Vyacheslav M. Zobin and Valeria I. Levina

Abstract A M_w 7.8 shallow subduction earthquake occurred on 5 December 1997 near Cape Kronotsky, Kamchatka Peninsula. Broadband *P*-wave inversions, carried out using two independent methods, allowed us to locate the position of the main asperities, one of high slip of up to 240 cm and a pair of lower slip, that ruptured during the mainshock. The mainshock hypocenter was located within the first asperity but not in the region of maximum slip. Most of the aftershock activity occurred within the low-slip asperities zone; the higher-slip asperity was characterized by low aftershock activity. All large aftershocks as well as the foreshocks ($M_w \geq 5.5$) occurred outside of the asperities. The mainshock was preceded by a long-term series of single moderate-size events. Based on the spatial distribution of preceding events, foreshocks, aftershocks, and two main asperity zones broken during the mainshock, the following fault history of the M_w 7.8 earthquake is proposed. There was an asperity zone below the Kronotsky Cape and its submarine continuation. This asperity was the site of concentration of the events preceding the mainshock, the single earthquakes of magnitude m_b between 5.5 and 6.1 that occurred during the 35 years before the mainshock of 5 December 1997. The M_w 5.8 earthquake of 9 February 1997, which was accompanied by aftershocks, finished this sequence of single events and marked a change in stress regime within the zone. A foreshock series occurred within the aftershock area of the 9 February earthquake, preparing the nucleus of rupture for the M_w 7.8 event, which began at the periphery of the Kronotsky asperity and then broke it almost completely. The rupture continued its way to the southwestern asperities. However, the southwestern asperities were only partially broken, with the amplitude of slip half that for the first asperity. As a result, during the aftershock stage, the maximum activity occurred around these asperity zones. The region of the first asperity, which was completely broken by the mainshock rupture, had almost no aftershock activity.

Introduction

The M_w 7.8 earthquake of 5 December 1997 occurred near Cape Kronotsky, Kamchatka Peninsula, in the northwestern part of the Pacific Ocean at the northern termination of the Kurile-Kamchatka subduction zone (Fig. 1). This large, thrust-type event was preceded and accompanied by numerous smaller events, forming a classical foreshock–mainshock–aftershock sequence, and was also preceded by a long-term series of moderate-size events. This earthquake was the strongest one within the Kamchatka portion of the Kurile-Kamchatka subduction zone since 1959.

Figures 2 and 3 show the main features of the foreshock–aftershock process. The foreshock events began on 3 December 1997, 46 hr before the mainshock. The foreshocks gradually increased in number, and the maximum number was observed a few hours before the mainshock. The foci of the events were distributed at depths from 0 to 40 km. The mainshock occurred at the southern border of the foreshock area at the depth of 10 km.

The maximum number of aftershocks was observed during the first 12 hr after the mainshock. Then the number of events gradually decreased, and by 9 December only 8–16 events were recorded in each 6-hr period. The aftershocks were distributed within an elliptical area with axes of 260-km and 120-km length situated along the slope of the oceanic trench between the 2000- and 5000-m isobaths (Fig. 1). The majority of the aftershocks was concentrated within the southwestern part of the aftershock area at a distance of about 100 km from the mainshock epicenter. The aftershock

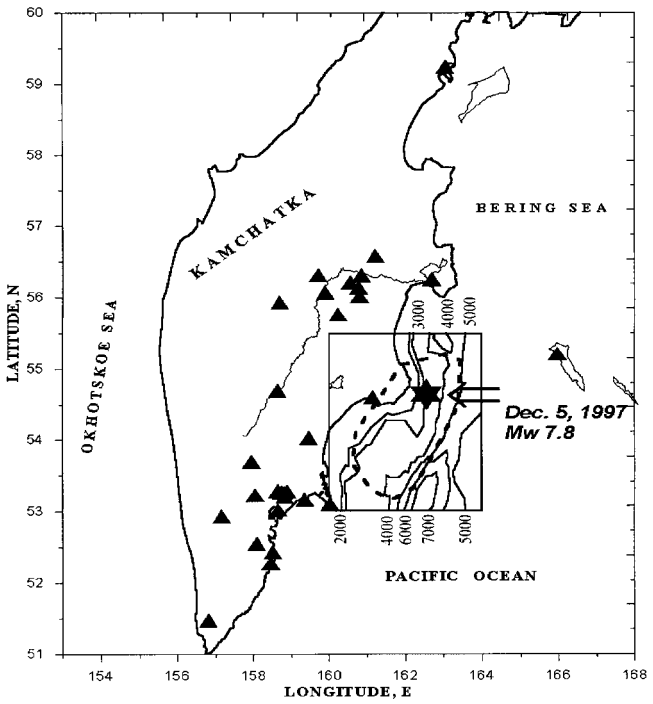

Figure 1. Study area and the Kamchatka seismic network. The study area is shown by a rectangle. The star shows the epicenter of the mainshock of 5 December 1997; the heavy dashed line shows the foreshock–aftershock area of the mainshock of 5 December. Seismic stations are shown by triangles. The bathymetry is shown from 2000 to 7000 m, with an interval of 1000 m.

distribution between the mainshock epicenter and the southwestern cluster was rather sparse. The aftershock hypocenters were located at depths from 0 to 50 km.

This article is devoted to the study of the earthquake source faulting process. We show that the earthquake had a complex history and discuss the comparative role of preceding events, foreshocks, the mainshock, and aftershocks in the process of breaking the fault. Following Ohnaka (1993), we consider the events preceding the mainshock as foreshocks if they occurred within about 10 days before the mainshock; the earlier events that occurred within the mainshock source area will be referred to as the preceding events. The article consists of two parts. In the first part, a model of the mainshock rupture is constructed; in the second part, the foreshock–aftershock process is compared with the location of the principal asperities broken by the earthquake.

Data and Methods

In our study we use the regional catalog of the events located by the Kamchatkan seismic network, the Harvard centroid-moment tensor (CMT) catalog, and the digital broadband records of the worldwide seismic networks.

The Kamchatkan seismic short-period network operated 31 stations (See Fig. 1) which allowed the location of all events of $M_s \geq 3.6$ during the foreshock–aftershock sequence and the majority of $M_s \geq 2.5$ events. The error in determination of the epicenter for these events, with locations by 9 to 29 stations (including the stations of the neighboring networks), was ± 5 km, while the depth error was ± 7 km. For the events of magnitude M_w 5.5 and greater (Table 1), located by 25 to 29 stations, the errors were ± 3.5 km and ± 4.0 km, respectively.

The CMT data (Table 1 and 2) were taken from the Harvard University Internet Data Base. The teleseismic digital records of broadband *P* waveforms were received by e-mail from the on-line services of the U.S. Geological Survey.

We analyzed the spatial distribution of foreshocks and aftershocks in comparison with the rupture history of the main event. The rupture history was reconstructed using two methods, the finite-fault *P*-waveform inversion of Hartzell and Heaton (1983) and the complex body-wave inversion of Kikuchi and Kanamori (1982). We call the corresponding models model I and model II, respectively. Both methods allow us to reconstruct the seismic moment release function; the first method gives the coseismic slip distribution along the fault plane, while the second method gives the spatial distribution of subevents along the fault. The simultaneous use of the two methods allows us to better constrain the rupture model.

P-Waveform Inversion of Mainshock and a Model of Mainshock Rupture

For the finite-fault modeling we used broadband data recorded by 12 stations and filtered with a bandwidth of 0.005–0.5 Hz. The record length was 100 sec, and all stations were situated at distances from 50° to 85°. The fault parameterization is presented in Table 3. The position of the hypocenter was taken from the Kamchatka Network catalog (Table 1), and then it was placed on the fault plane 75 km from the left edge of the fault and 14 km downward. A 2-sec-wide elementary boxcar source time function was used for each discrete rupture interval of each subfault. The width of the boxcar was chosen to be short compared to the rise time on the fault (Hartzell *et al.*, 1994). The inversion was conducted for up to 10 consecutive 2-sec time windows, which allows for a rise time of up to 20 sec. The crustal structure was the three-layer model used for the location of earthquakes by the Kamchatka regional seismic network (0–5 km, V_P 4.0 km/sec; 6–20 km, V_P 5.8 km/sec); 21–35 km, V_P 6.7 km/sec; 36–120 km, V_P 7.8 km/sec). The rupture velocity was set to 0.8 V_S in the layer containing the hypocenter, or 2.7 km/sec. The best solution for the rupture model was chosen by smoothing the solution with the simultaneous minimization of the seismic moment and the Euclidean norm $|\mathbf{b} - \mathbf{Ax}|$, which is the difference between the matrix of synthetics, $\mathbf{Ax}$, and the vector $\mathbf{b}$ containing the seismic observations. The inversion was carried out using programs developed by S. Hartzell and C. Mendoza and provided to us (personal comm., 1995).

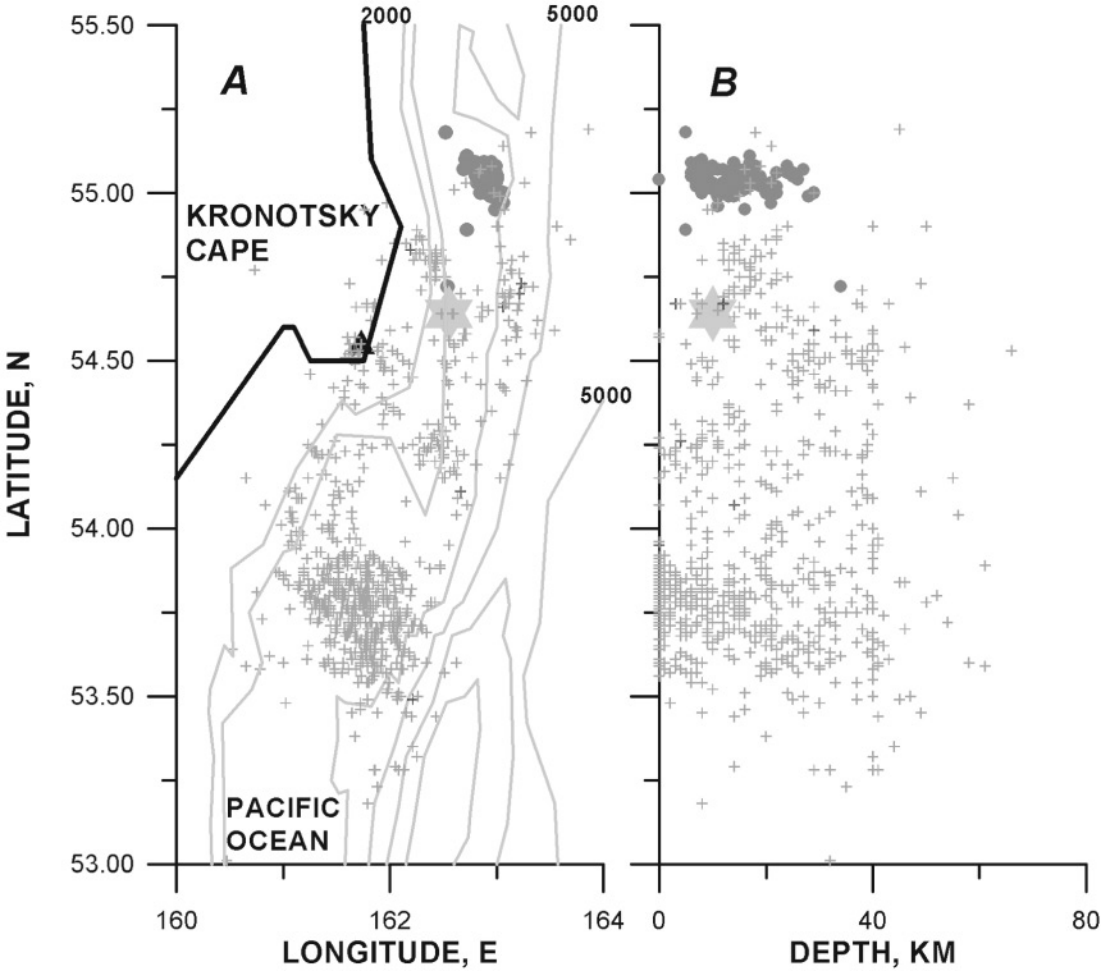

Figure 2. The distribution of (A) epicenters and (B) hypocenters of foreshocks (dots), mainshock (star), and aftershocks (crosses) of the M_w 7.8 earthquake of 5 December 1997, located during the first five days of activity. The events with magnitude $M \geq 2.6$ are shown. The isobaths are shown from 2000 to 7000 m with an interval of 1000 m. The triangle shows the position of the nearest seismic station.

Figure 4 shows the moment release function and the slip distribution corresponding to the model. The area of coseismic slip of 50 cm along the fault plane has a length of about 250 km and a width of about 120 km. Three zones of asperities are observed. The first, most intense one, with a slip of up to 240 cm, includes the hypocenter of the earthquake that was situated above the zone of main moment release. The rupture extends down and to the southwest from the 10-km-depth hypocenter with maximum slip at depths from 21 to 28 km. The second asperity zone is located about 100 km to the southwest from the hypocenter and includes a pair of smaller asperities. One of them, with a slip of up 130 cm, goes from the surface to a depth of 17 km, while the other, with a slip of up to 90 cm, is situated below the first at depths from 27 to 45 km. The third asperity is situated at depths from 48 to 54 km. Slips of up to 80 cm characterize it. The moment release function has a duration of about 80 sec. It is characterized by a low-intensity beginning during the first 5 sec, then a gradual increase with a maximum 20 sec after the beginning of rupture. The next maximum in moment release is observed at 40 sec. Then the process of moment release gradually decreased. The total seismic moment M_0 is equal to 7.2×10^{20} N m.

The model obtained (model I) was constrained by comparison with a model inferred from the complex body-wave inversion (M. Kikuchi, 1999, personal comm.). This model (model II) was based on the inversion of 20 broadband teleseismic *P* waveforms filtered with a bandwidth of 0.005–0.5 Hz and was constructed using the same velocity structure as for model I. The observed and synthetic seismograms and the rupture model are shown in Figure 5. The rupture model represents the moment rate function as well as the distribution of subevents along the fault plane. The subevents are shown as circles with radii proportional to the moment release. The total seismic moment, M_0, is equal to 3.5×10^{20} N m, which is one-half of the value obtained for model I.

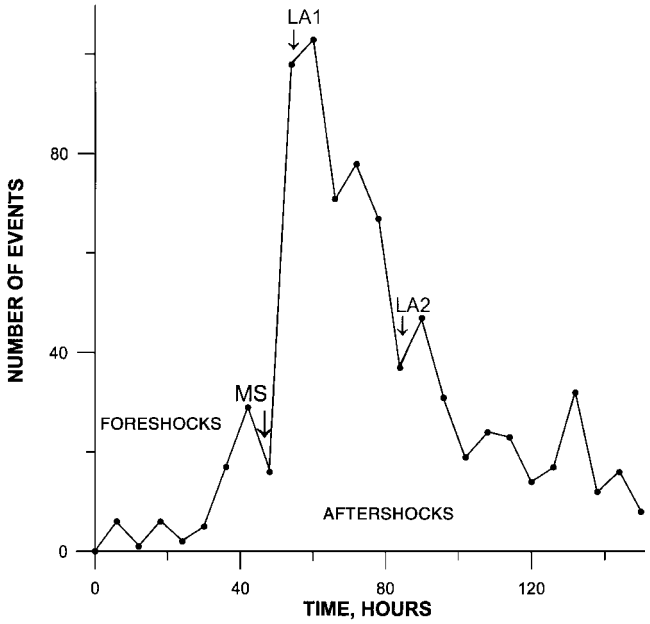

Figure 3. Temporal variation in the number of events during five days of the foreshock–mainshock–aftershock activity of the M_w 7.8 earthquake of 5 December 1997. The number of events with magnitude $M \geq 2.6$ is given for each 6-hr interval. The arrows give the time of the mainshock (MS) and two largest aftershocks (LA1, M_w 6.4 and LA2, M_w 6.2).

This value is also smaller than the values obtained by Maternovskaya and Ekstrom (1997) and Tanioka and Ruff (1997), equal to 5.3×10^{20} N m and 6.1×10^{20} N m, respectively. We attribute this difference in seismic moments for models I and II to the difference in smoothing procedures as well as to the difference in form and parameters of the source functions and rupture velocity used for the inversions. The difference in smoothing is clearly seen by comparison of the waveforms recorded at common stations (ARU and BORG) shown in Figures 4 and 5. The strong smoothing that partly deleted the details of short-period vibrations could explain the decrease of M_0 value and rather short moment release.

In spite of these differences, Figures 4 and 5 show that the two models are similar where they overlap. Figure 6 shows that the subevents of model II are distributed within two main asperity zones of model I with slip greater than 90 cm. Comparison of Figures 4 and 5 shows that the moment release functions for the two models are also similar for the first 60 sec of the process. Based on the relatively good agreement between the two models, we propose a rupture model with two asperity zones with slip greater than 90 cm and a moment release function with a duration of 60 sec. The deeper asperities of model I had slip of less than 90 cm and were excluded from the final model. We also conclude that the slip contours of the main asperities of model I can be used to reconstruct the rupture history. We take the 90-cm slip contours as the outlines of the asperities.

The Relationship between the Mainshock Asperities and the Preceding Events, Foreshocks, and Aftershocks

Preceding Events

The epicenter of the 5 December 1997 mainshock is situated between the Kurile-Kamchatka trench axis and the coast of Kamchatka near the 3000-m isobath (Figs. 1, 2). Figure 7 shows the epicenters of earthquakes with magnitudes 5.5 and greater that occurred after 1962 and prior to the 1997 mainshock. They are listed in Table 4. During 1962–1996, only single events occurred, but on 9 February 1997, this long-term sequence of single events was interrupted by the event of magnitude M_w 5.8, which was accompanied by aftershocks. Nine months later, the mainshock of 5 December occurred. The low threshold of the Kamchatka

Table 1
List of Events with $M_w \geq 5.5$

No.	Date (yymmdd)	Origin Time, (hhmmss.s)	Latitude (N)	Longitude (E)	Depth (km)	Seismic Moment (N m)	M_w
1	971204	224148.6	55.02	162.90	17	2.32×10^{17}	5.5
2	971205	080847.1	55.07	162.98	9	2.03×10^{17}	5.5
3	971205	112350.4	54.64	162.58	10	5.32×10^{20}	7.8
4	971205	184821.2	53.68	161.85	24	5.38×10^{18}	6.4
5	971206	002504.8	53.62	161.78	13	4.9×10^{17}	5.7
6	971206	063702.8	54.72	163.26	17	2.14×10^{17}	5.5
7	971206	063809.6	54.07	160.83	0	2.8×10^{17}	5.6
8	971206	100500.2	53.78	162.42	13	3.67×10^{17}	5.6
9	971206	105907.6	53.85	162.03	7	1.55×10^{18}	6.1
10	971206	123721.8	54.82	162.24	21	8.79×10^{17}	6.1
11	971207	175617.4	54.60	163.17	22	2.12×10^{18}	6.2
12	971207	230549.2	53.66	162.07	23	3.07×10^{17}	5.6
13	971208	210611.1	53.69	161.17	21	2.36×10^{17}	5.5

The origin times and hypocenters are taken from the Kamchatka Network catalog, the seismic moments and moment magnitudes are from the Harvard CMT catalog.

Table 2
Focal Mechanisms of Events
(Harvard CMT Best Double-Couple)

No.	Strike I (°)	Dip I (°)	Slip I (°)	Strike II (°)	Dip II (°)	Slip II (°)
1	187	27	63	36	66	103
2	185	22	64	32	71	100
3	202	23	74	39	68	97
4	212	19	104	17	72	85
5	177	32	67	24	61	104
6	192	32	68	38	60	103
7	202	33	75	39	58	100
8	198	25	75	35	66	97
9	204	26	75	41	65	97
10	204	28	93	20	62	88
11	205	15	81	35	75	93
12	214	29	107	15	63	81
13	217	32	89	37	58	90

Numbers as in Table 1.

Table 3
Parameterization of the Fault Model I

Parameter		Parameter	
Fault length (km)	250	Depth to the top of fault (km)	5
Fault width (km)	150	Depth to the bottom of fault (km)	63.6
Number of subfaults	225	Strike of fault (°)	202
Subfault length (km)	16.7	Dip of fault (°)	23
Subfault width (km)	10		

The strike and dip of the fault in the model I were taken from Table 2 (event No 3).

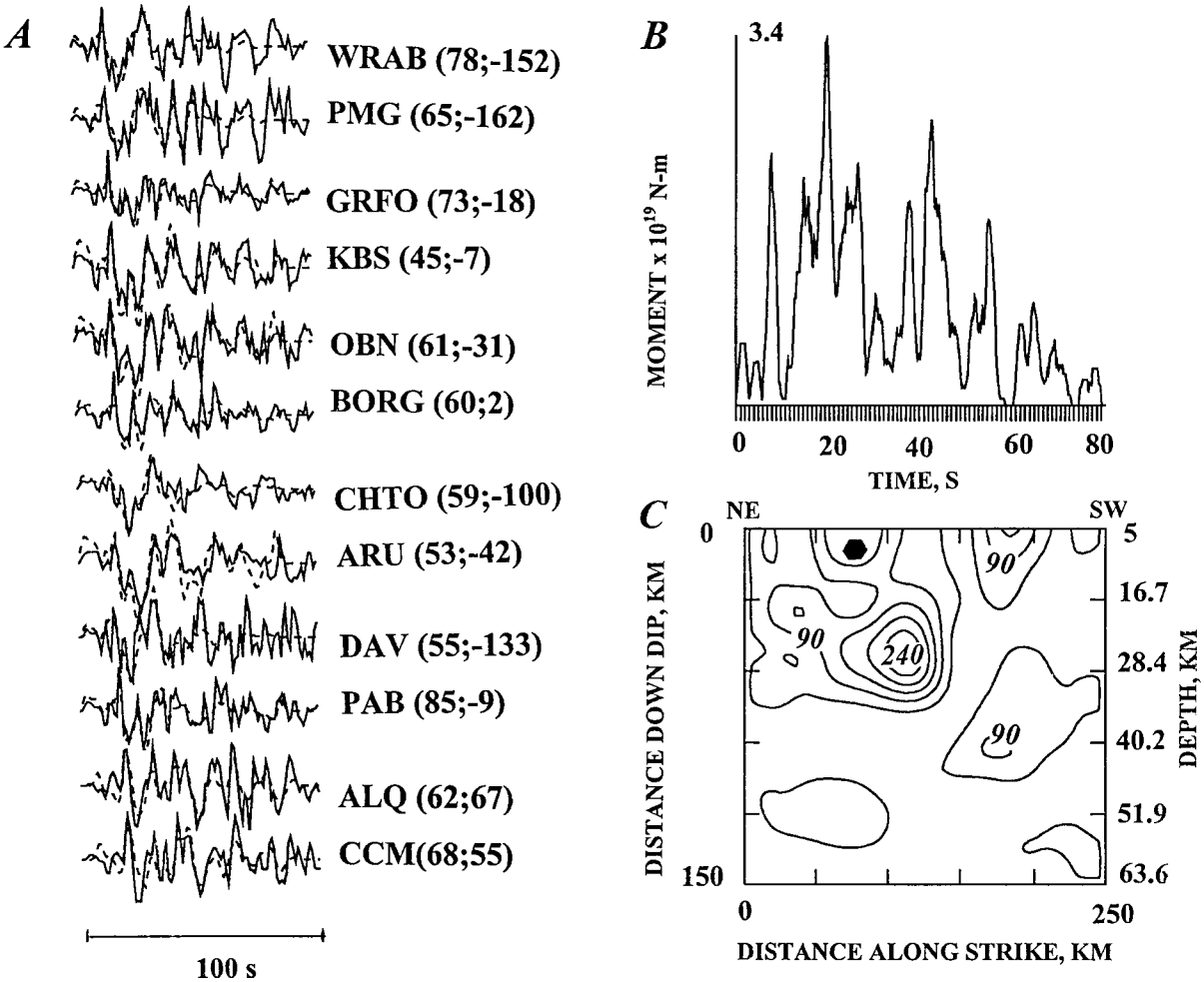

Figure 4. Results of the finite-fault *P*-waveform inversion for the mainshock (model I). (A) Comparison of observed (solid line) and synthetics (dashed line) waveforms. (B) Moment release function. (C) Final slip distribution along the fault plane. For each record, the name of the station, the epicentral distance, and the azimuth from epicenter, both in degrees, are given. The position of the hypocenter on the fault plane is shown by the hexagon. Cumulative slip is contoured at 40-cm intervals beginning from 50 cm. The original records were filtered with a bandwidth of 0.005–0.5 Hz. The synthetics were convolved with the instrument response.

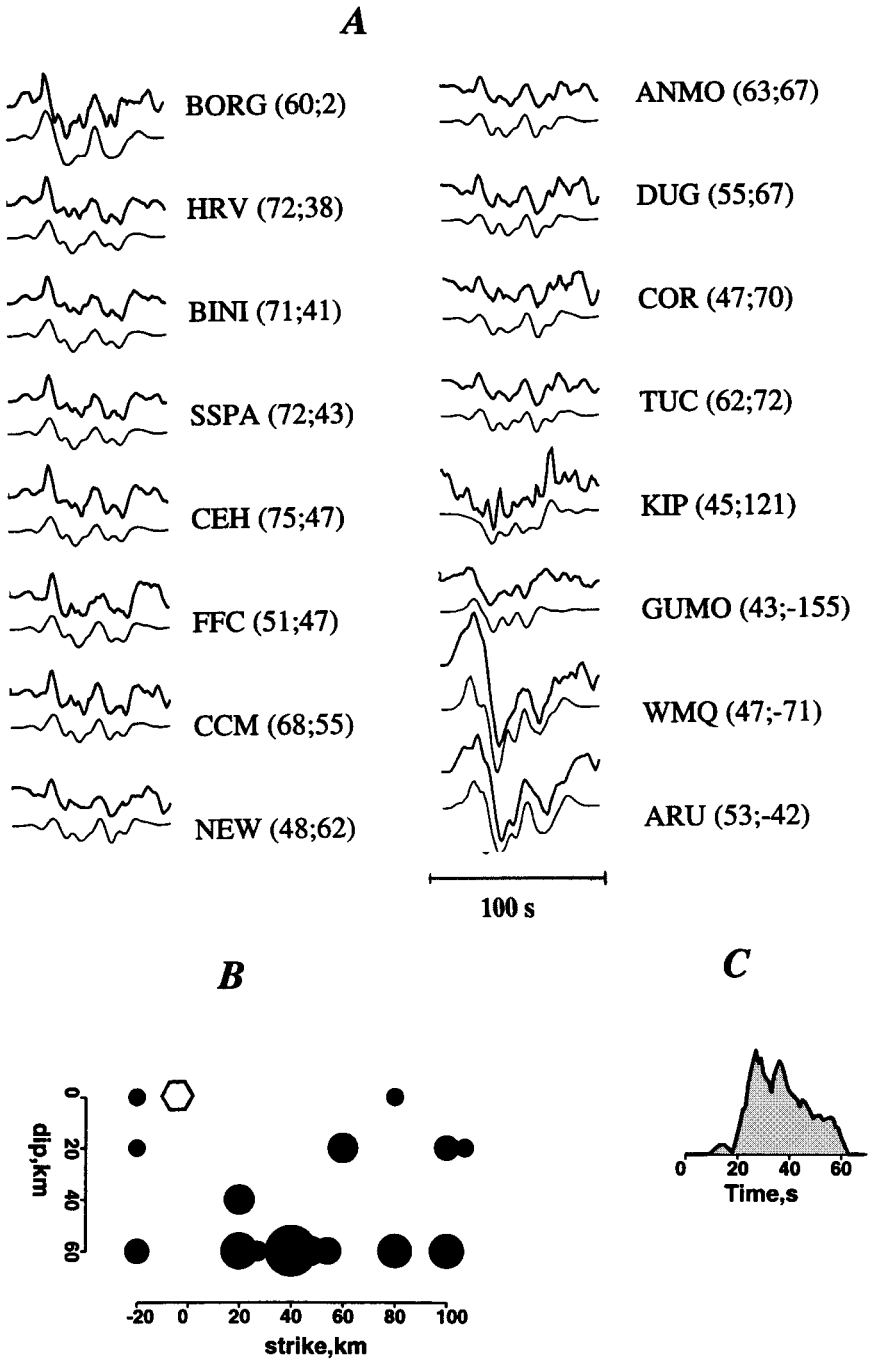

Figure 5. Results of the complex body-wave inversion for the mainshock (model II). Courtesy of M. Kikuchi. (A) Comparison of observed (heavy line) and synthetics (thin line) waveforms for 16 records. (B) Distribution of subevents along the fault plane. (C) Moment release function. For each record, the name of station, the epicentral distance, and the azimuth from epicenter (both in degrees) are given. Circles correspond to subevents with radii proportional to the moment release. The original records were filtered with a bandwidth of 0.005–0.5 Hz and converted to ground displacement.

catalog in 1964–1996 ($M \geq 2.5$) allowed to reveal this effect with high significance.

This occurrence of a large earthquake preceded by a moderate magnitude event accompanied by aftershocks (paired events) after a long period of single events is observed for almost all earthquakes with magnitudes M_w 6.9–7.1 that occurred in the last 35 yr within the shallow Kurile-Kamchatka subduction zone near the Kamchatka peninsula (Zobin, 1998).

The comparison of the hypocenters of the preceding

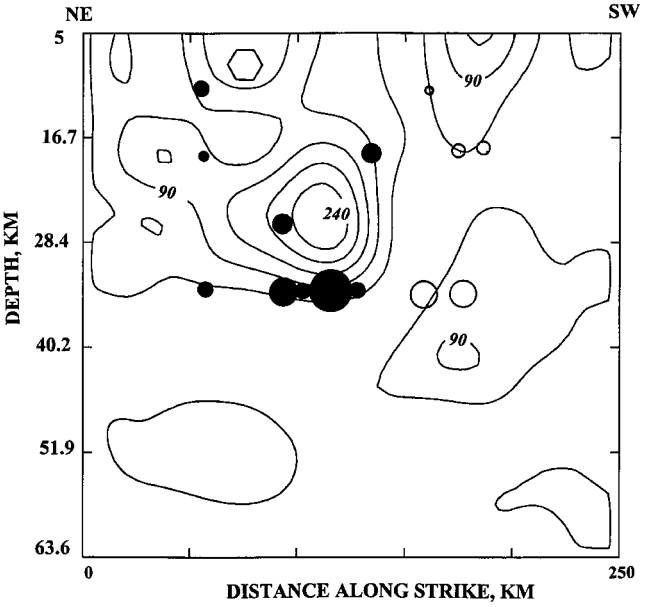

Figure 6. Comparison of model I and model II. Contours of slips from Figure 4C, corresponding to model I, and the subevents (filled and white circles) from Figure 5B, corresponding to model II, are shown. For better comparison, the subevents coincident with the largest asperity are shown by filled circles, while those situated along the second asperity zone are shown by open circles. The position of the hypocenter on the fault plane is shown by the hexagon.

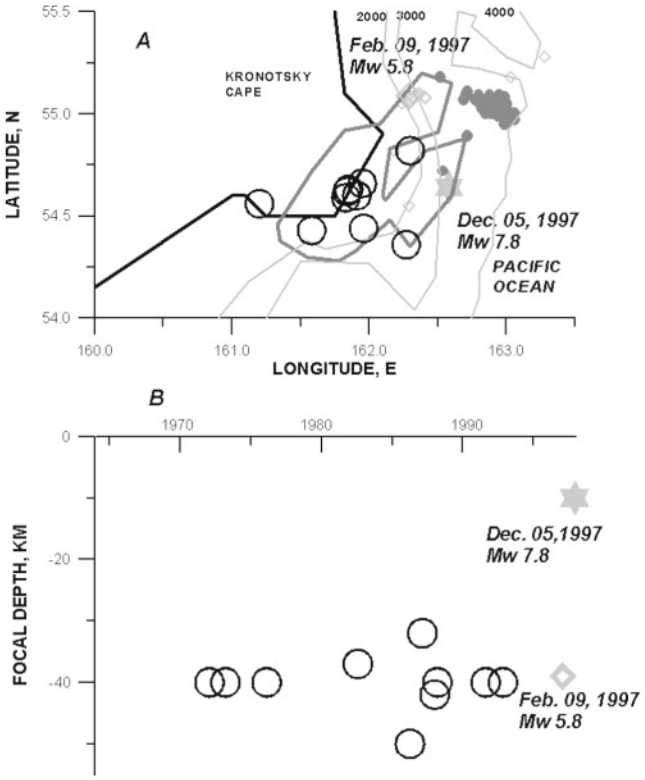

Figure 7. The seismic history prior to the M_w 7.8 earthquake of 5 December 1997 during 1962–1997. (A) Epicenters of the mainshock of 5 December (star), the single $m_b \geq 5.5$ earthquakes that occurred in 1962–1996 (open circles), the M_w 5.8 earthquake of 9 February 1997 (large diamond) and its aftershocks (small diamonds), and the foreshocks of the earthquake of 5 December (small filled circles). Also shown are the horizontal projection of the mainshock asperity of 5 December (heavy-line closed curve) and isobaths of the ocean floor. (B) Temporal distribution of single events (open circles) and the event with aftershock sequence (diamond) before the large earthquake of 5 December (star).

intermediate-size earthquakes and the location of the main asperity that ruptured during the mainshock of 5 December shows (Fig. 7) that the majority (9 out of 10) of the single events originated just below the asperity at depths from 32 to 50 km and that they outlined the area of main moment release of the forthcoming mainshock. The intermediate-size event followed by aftershocks occurred in the northern part of the asperity and near the foreshocks sites.

Foreshock and Aftershock Activity

Figure 8 shows the epicentral distribution of the foreshocks and aftershocks with $M_w \geq 5.5$ and the horizontal projections of the two main asperity zones that ruptured during the main fault. All foreshocks, including two large foreshocks (No. 1 and 2), occurred at the northern end of the rupture zone, outside the two asperity zones.

Small aftershocks occurred mainly within and around the southwestern asperities. The main asperity area was also filled by small aftershocks but in lesser amount. Large aftershocks occurred in two groups, outside of the areas of maximum slips but near the asperities. The first large aftershock was recorded 7 hr after the mainshock, whereas the last occurred 81 hr after the mainshock. The majority of the large aftershocks (7 out of 10) occurred within the southwestern portion of the aftershock area, whereas the remaining three events were located near the hypocenter of the mainshock. Table 2 shows that all large foreshock–aftershock events, including the mainshock, had a similar focal mechanism.

Figure 8 allows the comparison of the location of the main asperities ruptured by the mainshock with the location of large aftershocks. It is seen that the larger asperity with slip of 240 cm that was broken near the mainshock hypocenter is situated in the zone of sparse aftershock activity. The three large aftershocks of the northern part of the aftershock area were located outside of the asperity. On the contrary, the southwestern low-slip asperities are situated within the zone of high aftershock activity and are surrounded by large aftershocks.

Discussion and Conclusions

The broadband *P*-wave inversions, carried out using two independent methods, allowed us to locate the position

Table 4
List of the Events Preceding the Mainshock of 5 December 1997 ($m_b \geq 5.5$)

Date (year)	Date (mmdd)	Latitude (N)	Longitude (E)	Depth (km)	m_b	M_s	Type of Event
1972	0118	54.56	161.60	40	5.6	5.0	s
1973	0304	54.60	161.91	40	6.1	5.8	s
1976	0203	54.36	162.27	40	6.0	5.2	s
1982	0720	54.43	161.58	37	5.5	4.3	s
1986	0401	54.44	161.96	50	5.7	5.1	s
1987	0214	54.66	161.95	32	5.7	5.0	s
1988	0111	54.62	161.84	42	5.8	4.9	s
1988	0312	54.63	161.85	40	5.7	4.5	s
1991	0806	54.59	161.83	40	5.5	4.1	s
1992	1127	54.82	162.30	40	5.6	5.0	s
1997	0209	55.09	162.29	40	5.9	5.3	a

The magnitudes m_b and M_s were taken from *Monthly Listings of U.S. Geological Survey.* The type of event is indicated as s, single event; a, mainshock with aftershocks.

of main asperities, one of high slip of up to 240 cm, and a pair of lower slip, which ruptured during the mainshock of 5 December 1997. The mainshock hypocenter was located within the first asperity but not in the region of the maximum slip. Most of the aftershock activity occurred within the low-slip asperities zone; the higher-slip asperity was characterized by low aftershock activity. All large aftershocks as well as foreshocks ($M_w \geq 5.5$) occurred outside of the asperities. The mainshock was preceded by a long-term series of single events. Based on the spatial distribution of the preceding events, foreshocks, aftershocks, and two main asperities broken during the mainshock, a model for the source area can be constructed (Fig. 8).

Three distinct zones can be identified in the source area. Zone I forms the northern end of the area and represents the foreshock area. The intermediate zone II includes the hypocenter of the mainshock, the larger asperity zone, the epicenters of the preceding 1962–1997 earthquakes, and three

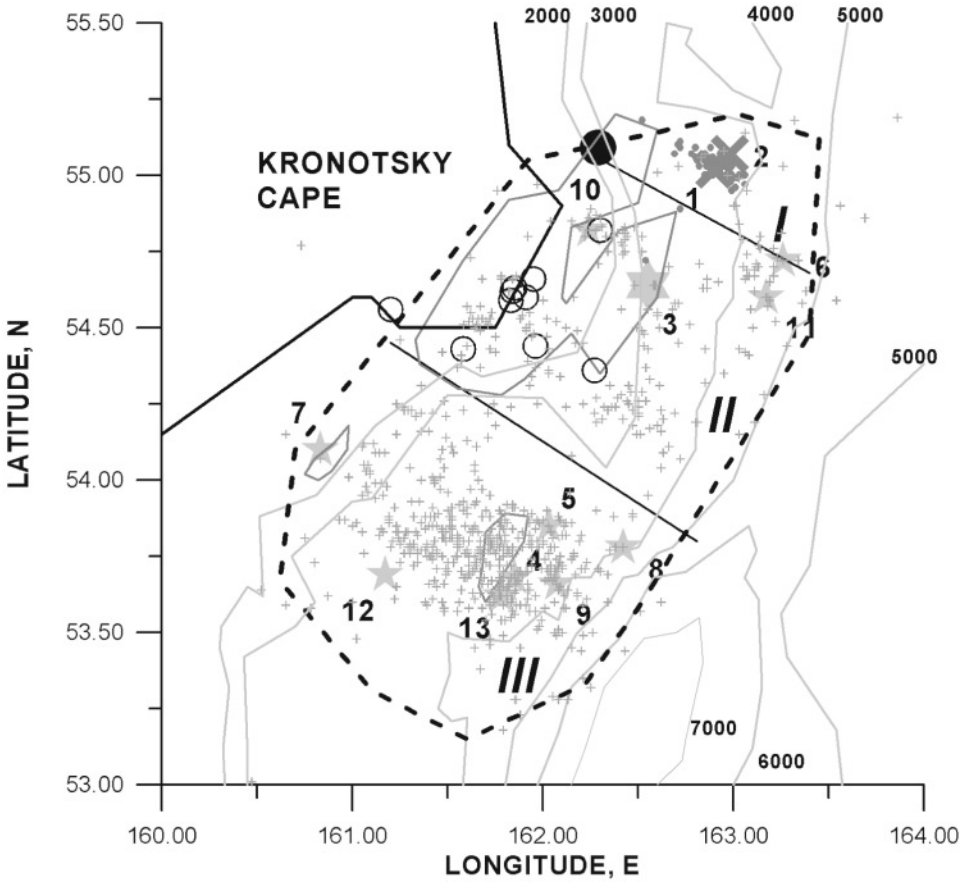

Figure 8. Comparative position of the horizontal projections of the asperities of the mainshock of the 5 December 1997 earthquake (heavy-line closed curves), foreshocks (filled circles), and aftershocks (crosses) with $M_w < 5.5$ and foreshocks (large crosses) and aftershocks (filled small stars) with $M_w \geq 5.5$. Also shown are the foreshock–aftershock area (dashed line), the epicenter of the mainshock (large star), the epicenters of moderatesized events that occurred in 1962–1967 (open circles) and the 9 February 1997 mainshock (large filled circle). The numbers by large seismic events correspond to the numbers of Table 1. Isobaths as in Figure 2. The Roman numerals I, II, and III, identify the three zones of the source area.

large aftershocks. This part of the rupture area represents the main zone of the moment release during the mainshock. The southwestern part of the source area, zone III, includes the smaller asperities zone, and the majority of the large aftershocks.

Based on these conclusions, the following fault history of the M_w 7.8 earthquake is proposed. There was an asperity zone below the Kronotsky Cape and its submarine continuation. This asperity was the site of concentration of the events preceding the mainshock, the single earthquakes of magnitude m_b from 5.5 to 6.1 that occurred in the 35 yr before the mainshock of 5 December 1997. The M_w 5.8 earthquake of 9 February 1997, which was accompanied by aftershocks, finished this sequence of single events and marked a change in stress regime within the zone. A foreshock series occurred within the aftershock area of the 9 February earthquake, preparing the nucleus of rupture for the M_w 7.8 event, which began at the periphery of the Kronotsky asperity and then broke it almost completely. The rupture continued its way to the southwestern asperities. However, the southwestern asperity zone was only partially broken, with the amplitude of slip half that for the first asperity. As a result, during the aftershock stage, the maximum activity occurred around this asperity. The region of the first asperity, which was completely broken by the mainshock rupture, had almost no aftershock activity.

Therefore, this model demonstrates the role of asperities in the process of nucleation and occurrence of large earthquake rupture. A long-lived asperity can be a place for a sequence of moderate-size earthquakes for a long time. Then a large earthquake can break the asperity. If this destruction is complete, the aftershocks are very few; if the rupture of asperity is only partial, intensive aftershock activity around the asperity zone is observed. It is important to note that larger aftershocks occurred outside of zones of maximum coseismic slip during the mainshock.

This model is in a good agreement with the results obtained for other large subduction earthquakes. Zobin (1996, 1998) showed the existence of preceding events for large Kamchatka earthquakes. They represent a sequence of single moderate-sized events, which were then followed by an intermediate event accompanied by aftershocks. Such a sequence preceded the M_w 7.0 earthquake of 8 August 1983 and the M_w 6.9 earthquakes of 2 March 1992 and 8 June 1993.

Hurukawa (1998) studied the foreshock–aftershock process related to the M_w 7.9 off-Etorofu (Iturup), Kurile Islands, earthquake of 3 December 1995. The model constructed by Hurukawa for this large event is close to ours. He showed that the foreshocks were concentrated at one end of the foreshock–aftershock zone (similar to our zone I), and the mainshock also occurred at the border between the foreshock and aftershock areas.

Our conclusions about the higher aftershock activity, which concentrated near the smaller asperity, partly ruptured during the mainshock, and the lower aftershock activity near the larger asperity, completely broken during the mainshock, are supported by many previous investigations of subduction earthquakes. The inversion for the mainshock of the M_w 7.9 off-Etorofu (Iturup), Kurile Islands, earthquake of 3 December 1995 (M. Kikuchi, personal comm., 1999) showed that the main moment release during the rupture of this earthquake occurred in about the first 40 sec with the asperity located about 60 km to the NE of the mainshock epicenter. The comparison of the aftershock distribution from Hurukawa (1998) and the location of the main asperity broken during the earthquake demonstrates that the majority of aftershocks occurred near the mainshock epicenter, where the relatively smaller asperities were not completely broken by the mainshock. However, in the region of the larger asperity, which was assumed completely broken by the mainshock, the aftershock activity was rather low.

The study of the M_w 7.6 Kushiro-oki, Hokkaido, earthquake of 15 January 1993, showed that the aftershock activity was low in the area of large slip that was predicted by the kinematic as well as the dynamic models of the rupture (Takeo *et al.*, 1993; Ide and Takeo, 1996). Most of the aftershocks were also observed outside of the region of large slip at the time of the mainshock of the M_w 7.7 Sanriku-Oki earthquake of 28 December 1994 (Nishimura *et al.*, 1996). Mendoza and Hartzell (1988) specially discussed the relationship between the asperity distribution and aftershock distribution along the mainshock fault and showed for the M_w 8.0 Michoacan, Mexico, earthquake of 19 September 1985, among others, that the aftershock clustering occurred near the edges, rather than within, the asperity zones.

Therefore, the model of earthquake rupture constructed for the M_w 7.8 5 December 1997 Kamchatka earthquake contains common features of the foreshock–aftershock process of shallow large subduction earthquakes.

Acknowledgments

Prof. M. Kikuchi kindly provided us with unpublished inversion data for the earthquakes of 3 December 1995 and of 5 December 1997. The comments made by Drs. K. Fujita, J. Pujol, and an anonymous reviewer were very valuable. This article was prepared while the first author was a Visiting Professor at the Earthquake Research Institute, Tokyo University.

References

Hartzell, S. H., and T. H. Heaton (1983). Inversion of strong ground motion and teleseismic waveform for the fault rupture history of the 1979 Imperial Valley, California, earthquake, *Bull. Seism. Soc. Am.* **73,** 1553–1583.

Hartzell, S. H., C. Langer, and C. Mendoza (1994). Rupture history of eastern North American earthquakes, *Bull. Seism. Soc. Am.* **84,** 1703–1724.

Hurukawa, N. (1998). The 1995 Off-Etorofu earthquake: joint relocation of foreshocks, the mainshock, and aftershock and implications for the earthquake nucleation process, *Bull. Seism. Soc. Am.* **88,** 1112–1126.

Ide, S., and Takeo, M. (1996). The dynamic rupture process of the 1993 Kushiro-oki earthquake, *J. Geophys. Res.* **101,** 5661–5675.

Kikuchi, M., and Kanamori, H. (1982). Inversion of complex body waves, *Bull. Seism. Soc. Am.* **72,** 491–506.

Maternovskaya, N., and G. Ekstrom (1997). Harvard CMT solution for 12/5/97, Harvard data base, *http://www.seismology.harvard.edu/CMTsearch.html* (last accessed November 2001).

Mendoza, C., and S. H. Hartzell (1988). Aftershock pattern and main shock faulting, *Bull. Seism. Soc. Am.* **78,** 1438–1449.

Nishimura, T., H. Nakahara, H. Sato, and M. Ohtake, (1996). Source process of the 1994 far east off Sanriku earthquake, Japan, as inferred from a broad-band seismogram, *Tohoku Geophys. J.* **34,** 121–134.

Ohnaka, M. (1993). Critical size of the nucleation zone of earthquake rupture inferred from immediate foreshock activity, *J. Phys. Earth* **41,** 45–56.

Takeo, M., S. Ide, and Y. Yoshida (1993). The 1993 Kushiro-oki, Japan, earthquake: a high stress drop event in a subducting slab, *Geophys. Res. Lett.* **20,** 2607–2610.

Tanioka, Y., and L. Ruff (1997). Source time function for 971205_Kamchatkevent, STF data base of University of Michigan, *http://www.geo.lsa.umich.edu/SeismoObs/STF.html* (last accessed November 2001).

Zobin, V. M. (1996). Earthquake clustering in shallow subduction zones: Kamchatka and Mexico, *Phys. Earth Planet. Interiors* **97,** 205–218.

Zobin, V. M. (1998). The paired earthquakes within the Kamchatka Peninsula subduction zone, *Tectonophysics* **289,** 341–350.

Observatorio Vulcanologico
Universidad de Colima
Colima, Col. 28045, México
vzobin@cgic.ucol.mx
(V.M.Z.)

Kamchatka Experimental and Methodological Department
Geophysical Service, Russian Academy of Sciences
9 Piip Av., Petropavlovsk-Kamchatskii, 683006, Russia
valeria@emsd.iks.ru
(V.I.L.)

Manuscript received 13 August 1999.